

Geophysical Research Letters°



RESEARCH LETTER

10.1029/2022GL099511

Key Points:

- A deep convolutional neural network (CNN) is trained to predict tsunami waveforms, based only on Global Navigation Satellite System (GNSS) data for hypothetical earthquakes
- Less than 9 min of data at GNSS stations selected from the existing dense network is used to predict 6 hr of tsunami waveforms
- Results compare favorably with a previous forecast model based on 30 or 60 min of tsunami waveform data

Supporting Information:

Supporting Information may be found in the online version of this article.

Correspondence to:

R. J. LeVeque, rjl@uw.edu

Citation:

Rim, D., Baraldi, R., Liu, C. M., LeVeque, R. J., & Terada, K. (2022). Tsunami early warning from Global Navigation Satellite System data using convolutional neural networks. *Geophysical Research Letters*, 49, e2022GL099511. https://doi. org/10.1029/2022GL099511

Received 9 MAY 2022 Accepted 8 OCT 2022

Author Contributions:

Conceptualization: Donsub Rim, Robert Baraldi, Christopher M. Liu, Randall J. LeVeque, Kenjiro Terada

Data curation: Donsub Rim, Robert Baraldi, Christopher M. Liu, Randall J. LeVeque

Formal analysis: Donsub Rim, Robert Baraldi

Funding acquisition: Kenjiro Terada Methodology: Donsub Rim, Robert Baraldi, Christopher M. Liu, Randall J. LeVeque, Kenjiro Terada

© 2022 The Authors.

This is an open access article under the terms of the Creative Commons Attribution-NonCommercial License, which permits use, distribution and reproduction in any medium, provided the original work is properly cited and is not used for commercial purposes.

Tsunami Early Warning From Global Navigation Satellite System Data Using Convolutional Neural Networks

Donsub Rim¹, Robert Baraldi², Christopher M. Liu³, Randall J. LeVeque^{3,4}, and Kenjiro Terada⁴

¹Deptartment of Mathematics and Statistics, Washington University in St. Louis, St. Louis, MO, USA, ²Sandia National Laboratories, Albuquerque, NM, USA, ³Department of Applied Mathematics, University of Washington, Seattle, WA, USA, ⁴International Research Institute of Disaster Science, Tohoku University, Sendai, Japan

Abstract We investigate the potential of using Global Navigation Satellite System (GNSS) observations to directly forecast full tsunami waveforms in real time. We train convolutional neural networks to use less than 9 min of GNSS data to forecast the full tsunami waveforms over 6 hr at select locations, and obtain accurate forecasts on a test data set. Our training and test data consists of synthetic earthquakes and associated GNSS data generated for the Cascadia Subduction Zone using the MudPy software, and corresponding tsunami waveforms in Puget Sound computed using GeoClaw. We use the same suite of synthetic earthquakes and waveforms as in earlier work where tsunami waveforms were used for forecasting, and provide a comparison. We also explore varying the number of GNSS stations, their locations, and their observation durations.

Plain Language Summary Producing rapid real-time forecasts for tsunamis in the first few minutes of an earthquake is a challenging problem. Accurate forecasts often rely on direct measurements of the tsunami, which are only available at sparse locations, and only after the tsunami has passed the sensors. Real-time numerical modeling of the tsunami is also time consuming. This work attempts to bypass these difficulties by considering a model that can forecast tsunami wave heights based only on Global Navigation Satellite System (GNSS) data, which is available within minutes from an extensive network of stations. We present some initial results using this approach for hypothetical tsunamis originating from the Cascadia Subduction Zone, with forecast locations in Puget Sound. We show that this approach gives comparable results to earlier work based on observing tsunami waveforms for 30 or 60 min, but now using only a few minutes of GNSS data. We explore varying the number of GNSS stations and find that the model yields accurate forecasts when as few as 20 GNSS stations are used, and outperforms our previous model when additional stations are used. The model performs well even when only the initial 4 min of GNSS data is used.

1. Introduction

Accurate tsunami early warning allows for more effective emergency planning, thereby mitigating the human and economic toll. However, constructing a rapid forecast model is challenging for several reasons. One is that the underlying physical processes are governed by partial differential equations whose solution requires substantial computation that cannot be performed in a short timeframe. Furthermore, determining the proper initial conditions for the differential equations requires solving the earthquake source inversion problem, which itself holds significant uncertainty due to the lack of direct observations. The current US warning system relies on early estimates of earthquake location and magnitude from seismic data, coupled with direct tsunami observations from Deep Ocean Assessment and Reporting of Tsunamis sensors (DART; Titov et al., 2005) in the deep ocean and coastal tide gauges. The sparsity of such sensors limits the amount of data one can collect on the tsunami directly. Moreover, one has to wait for the tsunami to reach these sensors, which can be hours after the earthquake.

In previous work (Liu et al., 2021a), hereafter referred to as Liu21, we explored machine learning (ML) techniques to forecast tsunami waveforms at two "forecast gauges" in the Puget Sound (denoted Gauges 901 and 911) shown in Figure 1. The forecasts were based on synthetic tsunami observations from Cascadia Subduction Zone (CSZ) events at an hypothetical "observation gauge" (denoted Gauge 702) in the Strait of Juan de Fuca. This ML approach avoids the need for real-time source inversion and tsunami simulation. We showed that several hours of tsunami waveforms at the forecast gauges could be forecast from shorter time series at the observation gauge, but it still requires 30–60 min of observed data after the tsunami reaches the observation gauge.

RIM ET AL.

Software: Donsub Rim, Robert Baraldi, Christopher M. Liu, Randall J. LeVeque **Supervision:** Donsub Rim, Randall J. LeVeque

Validation: Donsub Rim, Robert Baraldi, Christopher M. Liu, Randall J. LeVeque Visualization: Donsub Rim, Robert Baraldi, Christopher M. Liu, Randall J. LeVeque

Writing – original draft: Donsub Rim, Randall J. LeVeque

Writing – review & editing: Donsub Rim, Robert Baraldi, Christopher M. Liu, Randall J. LeVeque, Kenjiro Terada In this paper, we show that equally good forecasts can be made using only a few minutes of data from an existing network of Global Navigation Satellite System (GNSS) stations. Tsunami warning centers are already starting to incorporate this data in performing earthquake magnitude estimates, and it has been shown that the use of GNSS data can have great benefits, particularly for near-field forecasting (Crowell et al., 2018; Melgar, Allen, et al., 2016; Ohno et al., 2022; Ohta et al., 2018; Williamson et al., 2020). We show that this can be taken further by training Convolutional Neural Networks (CNNs) to forecast the tsunami waveforms directly from the GNSS waveforms. Recently ML has been applied to GNSS data in other approaches to tsunami warning, for example, to produce a model that rapidly estimates the earthquake magnitude (Lin et al., 2021), or as a supplement to ocean pressure sensor data to improve tsunami forecasts (Makinoshima et al., 2021; Tsushima et al., 2014). But to our knowledge this is the first demonstration of the potential for very rapid forecasting of accurate tsunami waveforms based only on a few minutes of GNSS data.

We consider the same forecast Gauges 901 and 911 as in Liu21, and use the same set of 959 CSZ events to train and test the ML model. In contrast to Liu21, our model input is now less than 9 min of GNSS data from a set of up to 60 GNSS stations (selected from a set of 62 stations shown in Figure 2). We show that this model does as well as the Liu21 model, despite using observation data that is available almost immediately after the earth-quake. Moreover, all 62 GNSS stations exist in practice (along with many more in the CSZ region), and there is a similar or greater density of GNSS stations in other active subduction zone regions such as Japan (Kawamoto et al., 2017) and Chile (Báez et al., 2018). Consequently, the methods studied here may be widely applicable to other subduction zones around the world.

2. GNSS and Tsunami Waveform Data Sets

The hypothetical earthquakes used for training the ML model are the same as those used in Liu21, which were taken from a set of 1,300 synthetic CSZ events that were generated by Melgar, LeVeque et al. (2016) and archived at (Melgar, 2016), and that range in magnitude from Mw 7.8 to 9.3. These realizations were generated using a Karhunen-Loève (KL) expansion as proposed by LeVeque et al. (2016) and implemented in the fakequakes module of the MudPy software (Melgar, 2020). We used the seafloor motion for each event as data for a tsunami simulation, performed using the GeoClaw software (Clawpack Development Team, 2020). Synthetic gauges placed at the gauge locations 702, 901, and 911 recorded the simulated tsunami over a 6 hr period. As in Liu21, from the set of 1,300 realizations we chose $N_{\rm data} = 959$ events with significant tsunamis, and used $N_{\rm train} = 613$ realizations (64%) in the training set, reserving $N_{\rm valid} = 154$ and $N_{\rm test} = 192$ realizations (16% and 20%) for the validation and test sets, respectively. All sets contained a random sample of events from the full range of magnitudes. Further details of the preparation appear in (Text S1 in Supporting Information S1).

The main contrast between this work and Liu21 is that our model now only utilizes the synthetic GNSS data from each of the events. This data at the 62 GNSS stations was computed with MudPy and archived at (Melgar, 2016); the original paper using this data focused on the use of GNSS data in the context of earthquake early warning.

Figure 2 shows the location of the 62 stations and a typical set of 20 stations chosen for training a model in our robustness study discussed below. The GNSS data for one sample realization #1127 at 10 of these stations is also shown to illustrate this data. Three channels (E, N, and Z) are recorded corresponding to ground motion in the east, north, and vertical direction, respectively. For plots of the slip, seafloor deformation, and tsunami propagation for this same realization #1127, see Liu21.

3. Methods

3.1. Forecast Model

Our forecast model is an ensemble of CNNs. Each CNN has an input variable of dimension $N_{\rm gnss} \times N_{\rm dir} \times N_{\rm in}$ and output variable of dimension $N_{\rm gauge} \times N_{\rm out}$. Here, $N_{\rm gnss}$ denotes the number of GNSS stations used for prediction, $N_{\rm dir}=3$ the number of GNSS channels (E, N, and Z), $N_{\rm in}$ the number of data points in the GNSS measurements (with a sampling rate of 1 Hz), $N_{\rm gauge}=3$, the total number of gauges where we make the forecast of the surface elevation, $N_{\rm out}=256$ the number of data points in computed tsunami surface elevation (tsunami waveform) over 6 hr. In our experiments, the choice of stations and $N_{\rm gnss}$ will be varied. To vary the number of seconds of observations used, we keep $N_{\rm in}$ fixed and mask the later values.

RIM ET AL. 2 of 9

1944807, 2022, 20, Downloaded from https://agupubs.onlinelibrary.wiley.com/doi/10.1029/2022GD99511 by Oregon State University, Wiley Online Library on [27032025]. See the Terms and Conditions (https://onlinelibrary.wiley.com/terms-and-conditions) on Wiley Online Library for rules of use; OA articles are governed by the applicable Creative

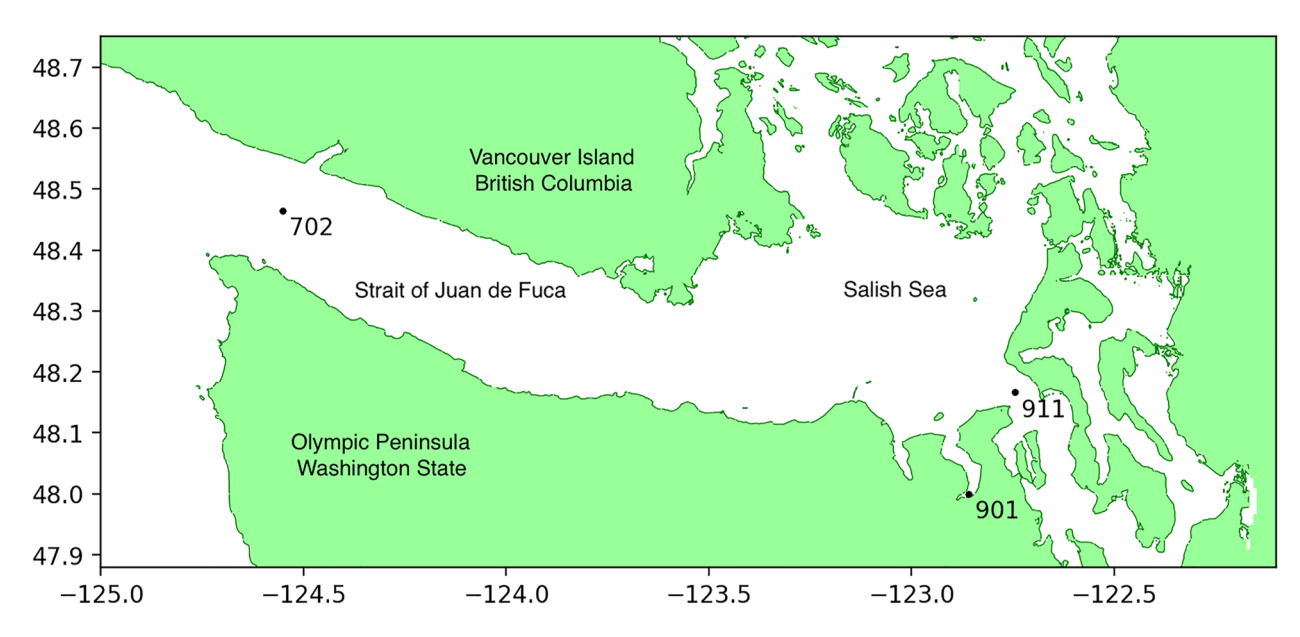


Figure 1. Strait of Juan de Fuca (SJdF) region with gauge locations. Gauge 702 is the hypothetical observation gauge used in Liu21, while Gauge 901 in Discovery Bay and 911 in Admiralty Inlet are the forecast gauges used both in that work and here. Reprinted with permission from Liu et al. (2021a).

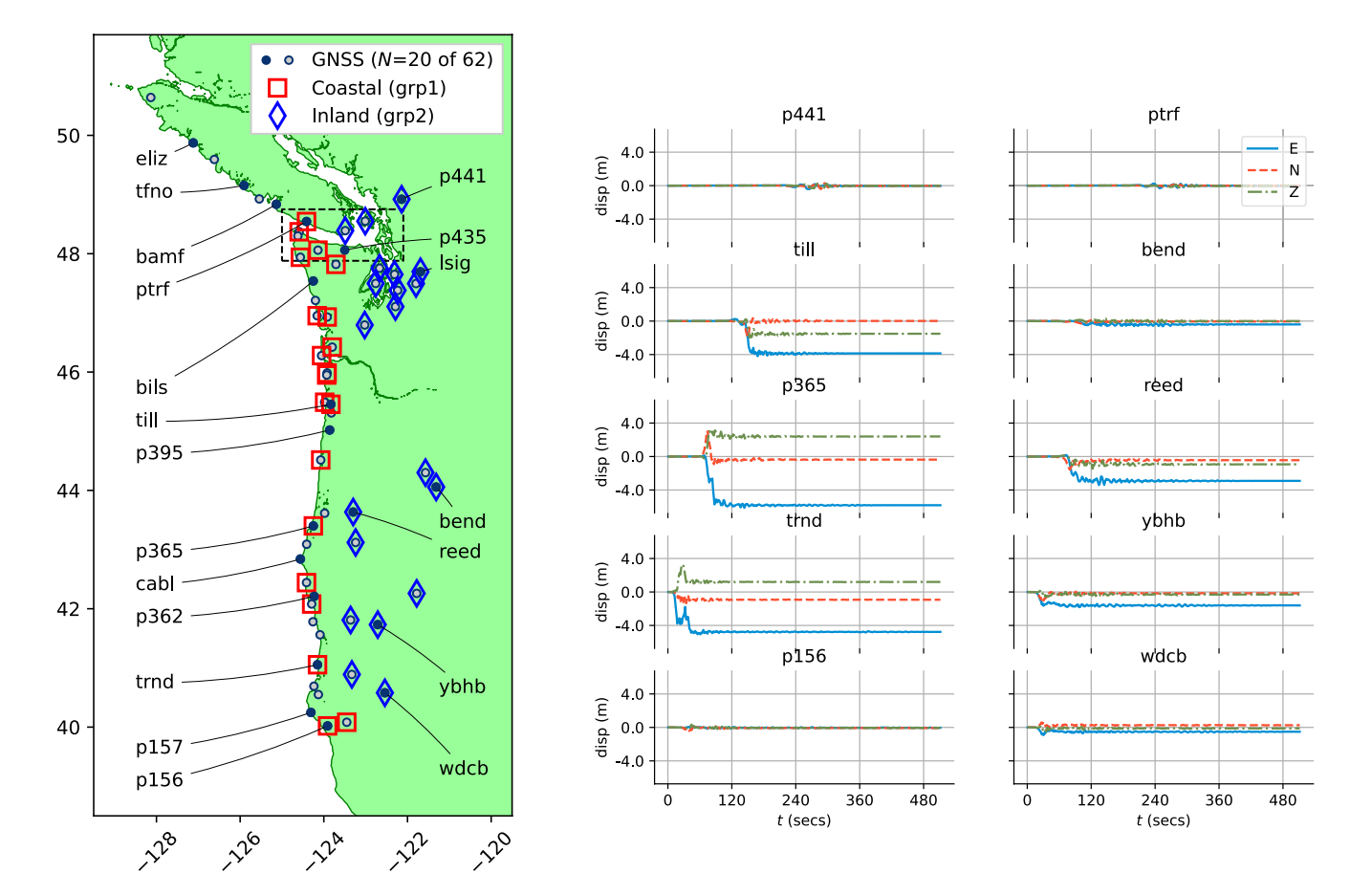


Figure 2. The map shows the location of 62 Global Navigation Satellite System (GNSS) stations, with a subset of 20 stations used in the sensor robustness study indicated with labels. The rectangle shows the study area from Figure 1. Sample GNSS data from 10 stations is shown on the right, for one Cascadia Subduction Zone earthquake Realization #1127. The red and blue symbols show the Group 1 and 2 stations discussed in the text, near the coast and inland, respectively. Up to 512 s of GNSS data is used to insure the full signal reaches all stations for all events.

RIM ET AL. 3 of 9

The CNN first applies a sequence of nine pairs of convolutional and max-pool layers, then applies the 8 transposed convolutional layers (Goodfellow et al., 2016). The CNN model is implemented and trained using the framework provided in the Python package pytorch (Paszke et al., 2019). Precise specifications of the model appear in Text S2 in Supporting Information S1.

3.2. Model Training

Our goal is to estimate the parameters of the CNNs by solving a standard optimization problem: with GNSS data as input, we minimize the L_1 error function between the CNN output and free surface time series as a function of the CNN parameters (Goodfellow et al., 2016); the L_1 error tends to prioritize larger magnitude events. In this minimization process, we can train the CNN by finding the parameters that best fit the data. This optimization is done using the stochastic gradient descent algorithm Adam (Kingma & Ba, 2015) with batch size 20 and fixed learning rate 10^{-4} . Rather than training a single CNN, we will train an ensemble made up of 25 CNNs. For each ensemble, we train CNNs individually via Adam until the validation error reaches a certain threshold.

3.3. Experiments

We perform three experiments. First, we conduct a sensor robustness study to explore the performance of the trained ensemble with respect to the number of GNSS stations used. We train six separate ensembles, with the number of GNSS stations used for input taken as $N_{\rm gnss} = 10, 20, ..., 60$. We randomly select a non-clustered subset of stations for each $N_{\rm gnss}$ (e.g., see Figure 2, full list in Table S1 in Supporting Information S1).

Second, we test how the observation duration affects the forecast performance. We vary the amount of GNSS data used by masking the input values after specified times $T_{\rm gnss}=120,240,360$ or 480s. When varying the observation duration, we use $N_{\rm gnss}=60$ stations throughout.

Third, we examine the effect that the sensor's distance to the fault may have on the performance. Among the GNSS stations south of 49° latitude we select two groups of $N_{\rm gnss} = 20$ stations: Group 1 stations lie along the coast, Group 2 farther inland (as shown in Figure 2).

4. Results

We carry out the training procedure using NVIDIA Tesla V100 SXM2 32 GB and it typically takes 90 min to complete training one ensemble. We provide the full details regarding the training in the supporting plots in Figures S1 and S2 in Supporting Information S1.

Selected forecast waveforms from the test set are shown in Figure 3 for the ensemble $N_{\rm gnss}=60$. For comparison, we include the predictions by the model developed in Liu21 based on 60 min of tsunami observation data from Gauge 702. The prediction error for Gauge 901 is expected to be higher than for 911 because of its location in Discovery Bay. The shallower 901 location corresponds to larger waves with more nonlinear behavior than the deeper water at Gauge 911. Figure 3 also shows Taylor diagrams (Taylor, 2001) summarizing the forecast results for both the other CNN ensembles that we trained in our robustness study ($N_{\rm gnss}=10,\ldots,60$), as well as those from Liu21. Taylor diagrams give a way of visualizing three measures of similarity between different time series, and have been used for this purpose in some other tsunami modeling studies, for example, (Lu et al., 2013). From these figures, we gather that the GNSS model exploiting input from all 60 stations performed the best.

Although the CNNs were trained using the L_1 error function, we additionally measure the skill of the CNN ensembles in predicting the maximum surface elevation η_{max} at each gauge, a primary quantity of interest in judging the magnitude of the tsunami at each location. To predict η_{max} , we simply compute the maximum of the forecast waveform of each individual model in the ensemble and use the mean as the predicted value. Plots demonstrating the forecast performance η_{max} are shown in Figures 4 and 5.

Figure 4 shows a plot of the mean absolute error and maximum absolute error, along with the L_1 test error for each ensemble. The L_1 test error and the error metrics for η_{max} follow similar trends. Figure 5 shows scatter plots of the forecast η_{max} versus the observed value (i.e., the value from the GeoClaw simulation) for each event in the test set. In general, both small and large tsunamis are forecast accurately. Also note that there are large magnitude events that created relatively small tsunamis at the gauge locations considered, and these are also predicted accurately.

RIM ET AL. 4 of 9

1944807, 2022, 20, Downloaded from https://agupubs.onlinelibrary.wiley.com/doi/10.1029/2022GL099511 by Oregon State University, Wiley Online Library on [27/03/2025]. See the Terms and Conditions (https://onlinelibrary.wiley.com/terms/

s-and-conditions) on Wiley Online Library for rules of use; OA articles are governed by the applicable Creative

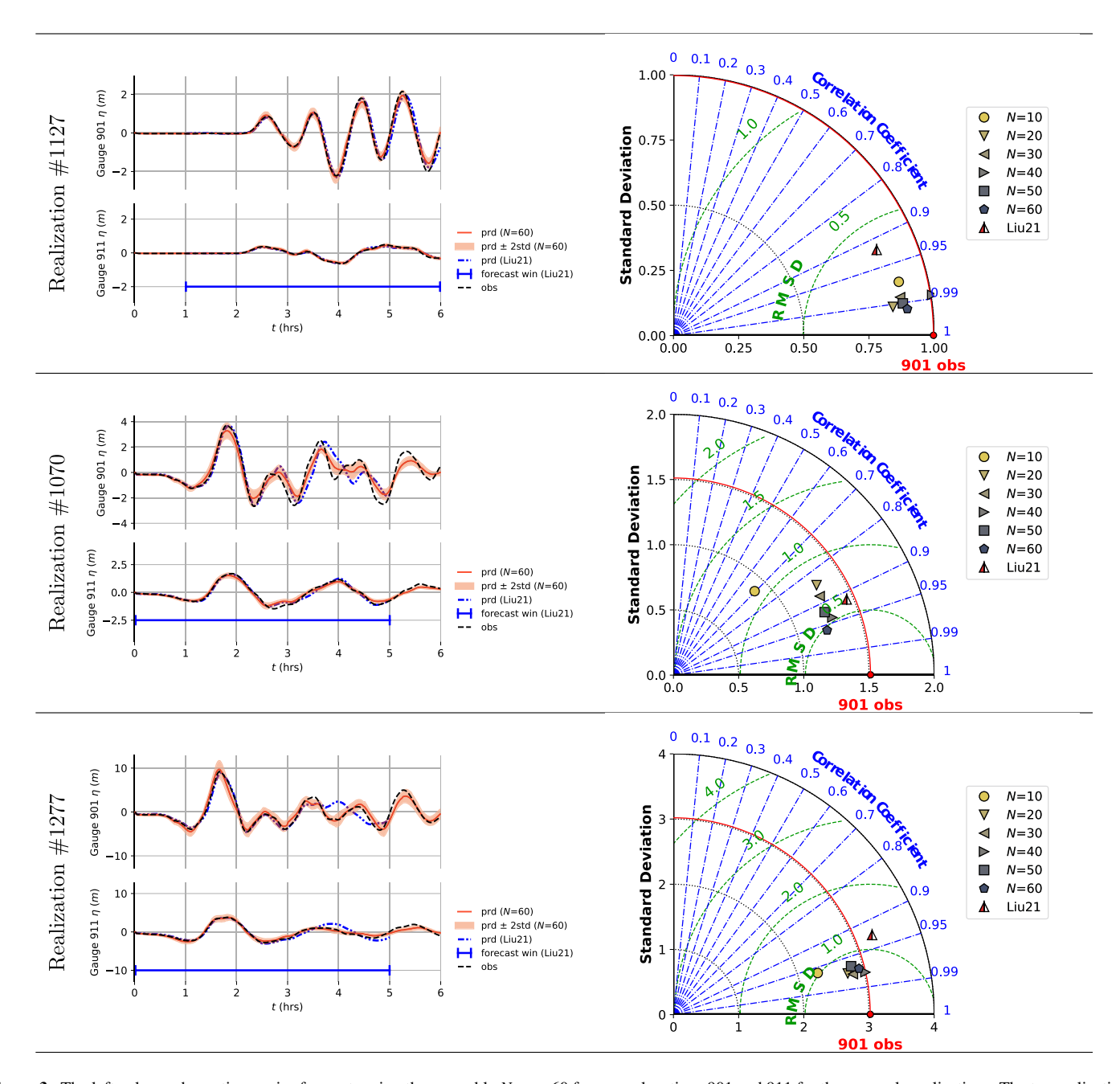


Figure 3. The left column shows time series forecasts using the ensemble $N_{\rm gnss} = 60$ for gauge locations 901 and 911 for three sample realizations. The top realization (#1127) was also illustrated in Liu21. The right column shows the Taylor diagram for each realizations for gauge 901, now comparing the results obtained using seven different machine learning predictions. Six of these use a varying number of Global Navigation Satellite System (GNSS) stations $N_{\rm gnss}$ from 10 to 60, while the point denoted by "Liu21" is the previous result for the 5-hr forecast window from Liu21, that used 60 min of tsunami waveform from Gauge 702 as input data. The Taylor diagram (e.g., Lu et al., 2013; Taylor, 2001) simultaneously shows the standard deviation of each waveform separately (radial distance), the root mean square error relative to the correct waveform (green contours), and the correlation coefficient between the forecast and correct waveforms (angular distance, blue contours). More accurate forecasts give points closer to the red dot.

In the data set used for these comparisons with Liu21, we filtered out events for which the tsunami signal was below a threshold, as described above. However, we obtain similar results when the model is trained and tested using the full unfiltered data set, as shown in (Text S3 in Supporting Information S1).

For the CNN ensembles trained in the sensor robustness study, the performance generally improves when more GNSS stations are used, but relatively little improvement of overall performance is seen beyond 20 stations and

RIM ET AL. 5 of 9

19448007, 2022, 20, Downloaded from https://agupubs.onlinelibrary.wiley.com/doi/10.1029/2022GL099511 by Oregon State University, Wiley Online Library on [27/03/2025]. See

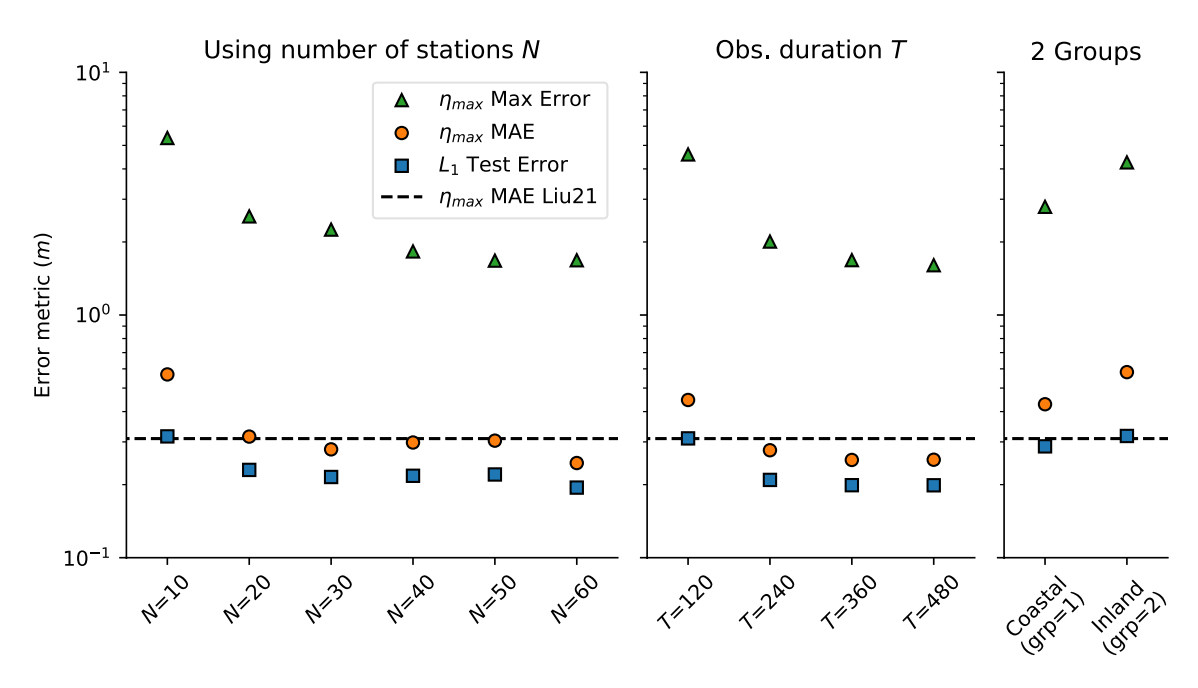


Figure 4. Model performance measured by comparing the maximum surface elevation η_{max} in the forecast waveform to that of the correct waveform, for each realization in the test set. The mean absolute error (MAE) and maximum error, as well as the L_1 test error are plotted. The MAE for model in Liu21 is also shown. Overall best result is obtained using all stations $N_{\text{enss}} = 60$ and all 512 s of Global Navigation Satellite System (GNSS) data.

this threshold agrees with the change in the decay behavior of the validation error. The sharpest decline in the performance of the model occurs when only 10 stations are used.

When 30 or more stations are used, we see increased overall performance of the CNNs trained with GNSS data than those reported in Liu21. This illustrates important practical advantages of using the GNSS data: we obtain a highly accurate forecast with data available within 9 min from the start of the tsunamigenic earthquake event, as opposed to 60 min after the tsunami starts to enter the Strait as required in Liu21, potentially a 2-hr difference. Moreover, these GNSS stations actually exist and are operational. This makes the new model a more suitable candidate for use in an early warning system.

The ensembles using varying observation durations show that the performance is not significantly affected when only the first 240s of GNSS data is used, suggesting that accurate forecast is possible within 4 min. The duration required for other locations will naturally depend on the distance from the fault to the GNSS stations and the duration of the earthquake events of interest. However, in general this duration will be on the order of minutes rather than the hours often require to obtain direct tsunami observations.

The results from ensembles using two different groups of 20 stations show that using only the stations that are situated inland at a significant distance from the fault causes the performance to deteriorate, especially for larger events (Figure 5). This suggests the model relies significantly on the measurements closer to the fault. But also note that both perform worse than when an equal number of well-distributed stations are used ($N_{\rm gnss} = 20$), suggesting that the inland stations also provide useful information. A sensitivity study using projected gradients supports these findings (Text S4 in Supporting Information S1).

5. Conclusions

We have developed a CNN model that uses less than 9 min of GNSS observations at existing onshore stations near the CSZ to produce a 6-hr forecast of the resulting tsunami waveforms at several gauge locations. These gauge locations agree with those used in our previous work denoted Liu21 (Liu et al., 2021a). We demonstrate that this GNSS-based approach works as well as our previous model input of 30 or 60 min of the tsunami waveform observed at a hypothetical gauge. We conclude that this approach is very promising for use in real-time warning systems and deserves further development.

RIM ET AL. 6 of 9

1944807, 2022, 20, Downoaded from https://agupubs.onfinelibrary.wiele.com/doi/10.1029/2022GL099511 by Oragon State University, Wiley Online Library on [27032025]. See the Terms and Conditions (https://onlinelibrary.wiley.com/terms-and-conditions) on Wiley Online Library for rules of use; OA articles are governed by the applicable Creative

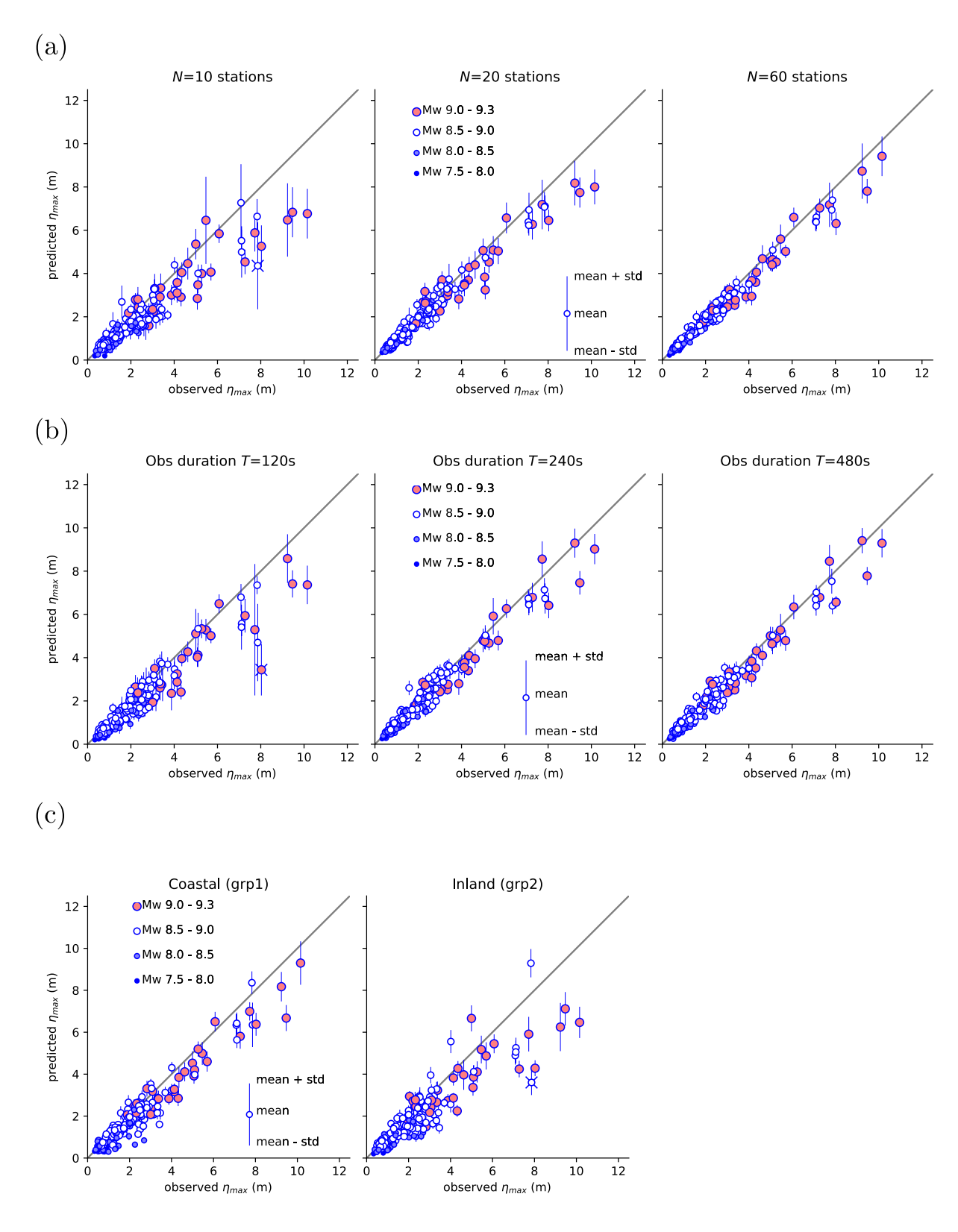


Figure 5. The scatter plots of the predicted η_{max} (the maximum surface elevation at the gauge 901 over the full time series) versus the correct value for each realization in the test set, for ensembles trained on (a) $N_{\text{gnss}} = 10$, 20, 60 stations, (b) observation durations $T_{\text{gnss}} = 120$, 240, 480s, (c) the two stations groups. In each row the prediction with worst error is marked by \times , and sensitivity studies for these cases appear in Supporting Information S1 (Text S4).

RIM ET AL. 7 of 9

19448007, 2022, 20, Downloaded

Several aspects of our work require additional research that is currently underway. We chose gauge locations in Puget Sound, WA for our study in Liu21 with the idea that observations at a single gauge (e.g., our Gauge 702) at the entrance of the Strait of Juan de Fuca might be sufficient to produce good forecasts in Puget Sound. That was important since there are currently no suitable observation gauges in this region and deploying even one gauge would be expensive. In this work, we used the same gauge locations in order to compare forecasts with our previous results; however, the existence of numerous GNSS stations in the region warrants further exploration of our model's ability to train and generate forecasts at other locations. We are currently collaborating with researchers at the NOAA Center for Tsunami Research to explore the ability of these ML models to provide both nearfield warnings for a CSZ event and also to potentially complement the existing farfield forecasting capabilities based on DART data. In addition to further experiments based on CSZ events, we are working with other researchers at Tohoku University to experiment with forecasting Nankai Trough events.

Our tests have all been performed so far with the synthetic GNSS data produced by the fakequakes software, without the addition of any noise. Real GNSS data can be quite noisy and it will be important to assess the robustness of this ML approach to noisy data. The synthetic GNSS waveforms are based on a simplified model of the earth's structure; we plan to explore how robust our CNN model is to synthetic data produced with a different model of the earth. This acts as a step toward exploring how well a model trained on synthetic data would forecast a real tsunami when the input data is from actual GNSS observations.

Data Availability Statement

The software for all numerical experiments performed in this work is available at https://github.com/dsrim/ML_GNSS_SJdF_2022 under the BSD-3 license. The earthquake realizations used in this paper were generated by Melgar, LeVeque et al. (2016) and archived at (Melgar, 2016). The tsunami waveforms for each realizations were generated using the GeoClaw Software (Clawpack Development Team, 2020), and available at (Liu et al., 2021b).

References

Báez, J. C., Leyton, F., Troncoso, C., del Campo, F., Bevis, M., Vigny, C., et al. (2018). The Chilean GNSS network: Current status and progress toward early warning applications. Seismological Research Letters, 89(4), 1546–1554. https://doi.org/10.1785/0220180011

Clawpack Development Team. (2020). Clawpack software. Retrieved from http://www.clawpack.org

Crowell, B. W., Melgar, D., & Geng, J. (2018). Hypothetical real-time GNSS modeling of the 2016 Mw 7.8 Kaikoura Earthquake: Perspectives from ground motion and tsunami inundation prediction. *Bulletin of the Seismological Society of America*, 108(3B), 1736–1745. https://doi.org/10.1785/0120170247

Goodfellow, I., Bengio, Y., & Courville, A. (2016). Deep learning. MIT Press. Retrieved from http://www.deeplearningbook.org

Kawamoto, S., Ohta, Y., Hiyama, Y., Todoriki, M., Nishimura, T., Furuya, T., et al. (2017). REGARD: A new GNSS-based real-time finite fault modeling system for GEONET. *Journal of Geophysical Research: Solid Earth*, 122, 1324–1349. https://doi.org/10.1002/2016JB013485
Kingma, D. P., & Ba, J. (2015). Adam: A method for stochastic optimization. In *International Conference for Learning Representations*. Retrieved from http://arxiv.org/abs/1412.6980

LeVeque, R. J., Waagan, K., González, F. I., Rim, D., & Lin, G. (2016). Generating random earthquake events for probabilistic tsunami hazard assessment. *Pure and Applied Geophysics*, 173(12), 3671–3692. https://doi.org/10.1007/s00024-016-1357-1

Lin, J.-T., Melgar, D., Thomas, A. M., & Searcy, J. (2021). Early warning for great earthquakes from characterization of crustal deformation patterns with deep learning. *Journal of Geophysical Research: Solid Earth*, 126, e2021JB022703. https://doi.org/10.1029/2021JB022703

Liu, C. M., Rim, D., Baraldi, R., & LeVeque, R. J. (2021a). Comparison of machine learning approaches for tsunami forecasting from sparse observations. *Pure and Applied Geophysics*, 178(12), 5129–5153. https://doi.org/10.1007/s00024-021-02841-9

Liu, C. M., Rim, D., Baraldi, R., & LeVeque, R. J. (2021b). Comparison of machine learning approaches for tsunami forecasting from sparse observations. [Datasets]. Zenodo. https://doi.org/10.5281/zenodo.5156748

Lu, W., Jiang, Y., & Lin, J. (2013). Modeling propagation of 2011 Honshu tsunami. Engineering Applications of Computational Fluid Mechanics, 7(4), 507–518. https://doi.org/10.1080/19942060.2013.11015489

Makinoshima, F., Oishi, Y., Yamazaki, T., Furumura, T., & Imamura, F. (2021). Early forecasting of tsunami inundation from tsunami and geodetic observation data with convolutional neural networks. *Nature Communications*, 12(1), 2253. https://doi.org/10.1038/s41467-021-22348-0 Melgar, D. (2016). Cascadia FakeQuakes waveform data and scenario plots. [Dataset]. Zenodo. https://doi.org/10.5281/zenodo.59943

Melgar, D. (2020). Mudpy. Retrieved from https://github.com/dmelgarm/MudPy

Melgar, D., Allen, R. M., Riquelme, S., Geng, J., Bravo, F., Báez, J. C., et al. (2016). Local tsunami warnings: Perspectives from recent large events. Geophysical Research Letters, 43(3), 1109–1117. https://doi.org/10.1002/2015GL067100

Melgar, D., LeVeque, R. J., Dreger, D. S., & Allen, R. M. (2016). Kinematic rupture scenarios and synthetic displacement data: An example application to the Cascadia Subduction Zone. *Journal of Geophysical Research: Solid Earth*, 121, 6658–6674. https://doi.org/10.1002/2016jb013314

Ohno, K., Ohta, Y., Hino, R., Koshimura, S., Musa, A., Abe, T., & Kobayashi, H. (2022). Rapid and quantitative uncertainty estimation of coseismic slip distribution for large interplate earthquakes using real-time GNSS data and its application to tsunami inundation prediction. *Earth Planets and Space*, 74(1), 24. https://doi.org/10.1186/s40623-022-01586-6

Ohta, Y., Inoue, T., Koshimura, S., Kawamoto, S., & Hino, R. (2018). Role of real-time GNSS in near-field tsunami forecasting. *Journal of Disaster Research*, 13(3), 453–459. https://doi.org/10.20965/jdr.2018.p0453

Acknowledgments

States Government.

Diego Melgar generated the hypothetical earthquakes used in this work and provided advice on the best use of GNSS data. The authors are also grateful to Xinsheng Qin for setting up and performing the GeoClaw simulations used as training and test data. Responding to the comments and questions of two anonymous referees led to significant improvements in this paper. RJL and CML were supported in part by Tohoku University. This research was sponsored by the Department of Energy Office of Science under the Advanced Scientific Computing Research John von Neumann Fellowship, Sandia National Laboratories is a multimission laboratory managed and operated by National Technology and Engineering Solutions of Sandia, LLC., a wholly owned subsidiary of Honeywell International, Inc., for the U.S. Department of Energy's National Nuclear Security Administration under contract DE-NA0003525. This paper describes objective technical results and analysis. Any subjective views or opinions that might be expressed in the paper do not necessarily represent the views of the U.S. Department of Energy or the United

RIM ET AL. 8 of 9

- Paszke, A., Gross, S., Massa, F., Lerer, A., Bradbury, J., Chanan, G., et al. (2019). Pytorch: An imperative style, high-performance deep learning library. In H. Wallach, H. Larochelle, A. Beygelzimer, F. d'Alché Buc, E. Fox, & R. Garnett (Eds.), *Advances in neural information processing systems 32* (pp. 8024–8035). Curran Associates, Inc.
- Taylor, K. E. (2001). Summarizing multiple aspects of model performance in a single diagram. *Journal of Geophysical Research*, 106(D7), 7183–7192. https://doi.org/10.1029/2000JD900719
- Titov, V. V., Gonzalez, F. I., Bernard, E. N., Eble, M. C., Mofjeld, H. O., Newman, J. C., & Venturato, A. J. (2005). Real-time tsunami forecasting: Challenges and solutions. *Natural Hazards*, 35(1), 35–41. https://doi.org/10.1007/s11069-004-2403-3
- Tsushima, H., Hino, R., Ohta, Y., Iinuma, T., & Miura, S. (2014). tFISH/RAPiD: Rapid improvement of near-field tsunami forecasting based on offshore tsunami data by incorporating onshore GNSS data. *Geophysical Research Letters*, 41(10), 3390–3397. https://doi.org/10.1002/2014GL059863
- Williamson, A. L., Melgar, D., Crowell, B. W., Arcas, D., Melbourne, T. I., Wei, Y., & Kwong, K. (2020). Toward near-field tsunami forecasting along the Cascadia subduction zone using rapid GNSS source models. *Journal of Geophysical Research: Solid Earth*, 125, e2020JB019636. https://doi.org/10.1029/2020JB019636

References From the Supporting Information

Selvaraju, R. R., Cogswell, M., Das, A., Vedantam, R., Parikh, D., & Batra, D. (2017). Grad-CAM: Visual explanations from deep networks via gradient-based localization. In *Proceedings of the IEEE International Conference on Computer Vision (ICCV)*.

RIM ET AL. 9 of 9